Available online at www.sciencedirect.com
ScienceDirect
Applied Geochemistry 23 (2008) 454–466
Applied Geochemistry
www.elsevier.com/locate/apgeochem

Sensitivity of the global atmospheric cycle of mercury to emissions

Kristen Lohman [a,*], Christian Seigneur [a], Mae Gustin [b], Steve Lindberg [c,1]

[a] Atmospheric and Environmental Research, Inc., 2682 Bishop Drive, Suite 120, San Ramon, CA, USA
[b] Department of Natural Resources and Environmental Science, University of Nevada, Reno, NV, USA
[c] Emeritus Fellow, Oak Ridge National Laboratory, Oak Ridge, TN, USA

Available online 11 January 2008

Abstract

A systematic investigation of the impact of current uncertainties in Hg emissions from specific source categories on global air Hg concentrations is presented. First, the uncertainties in different emission source categories are discussed and then the results of a base simulation and three sensitivity simulations conducted with a global chemical transport model for mercury (CTM-Hg) are presented. The total Hg emissions in the four scenarios range from 6600 to 9400 Mg/a. The sensitivity studies investigate the impact of the range in uncertainty in natural emissions, emissions of previously deposited Hg, and anthropogenic emissions both in China and worldwide, while taking into account constraints imposed by available data (current/pre-industrial emission ratio of 2–4). In one case, natural emissions and emissions of previously deposited Hg were changed to represent a mid point of the range of values found in the literature. This lead to a 16% increase in background emissions, i.e., natural emissions and emissions of previously deposited Hg combined. Increasing natural emissions by 16% or Chinese anthropogenic emissions by 100% yielded atmospheric Hg concentrations comparable with those measured across the globe without any changes to the atmospheric chemistry. Increasing natural emissions and emissions of previously deposited Hg by 16% and all anthropogenic emissions by 100% as compared to the base scenario yielded atmospheric Hg concentrations that were not compatible with measurements and changes in the chemical behavior of Hg in the atmosphere would be required to yield results that are consistent with observed Hg concentrations. The current uncertainty in total Hg emissions at the global scale is placed at about a factor of two.

1. Introduction

Current simulations of atmospheric Hg use a global total emission flux on the order of 6000 Mg/a (e.g., Bergan et al., 1999; Seigneur et al., 2004). There are, however, large uncertainties in those emissions (e.g., Lindberg et al., 2004, 2007; Gustin and Lindberg, 2005) and it is, therefore, of interest to understand how current understanding of the global Hg cycle can be affected by such uncertainties. In this work, the AER/EPRI chemical transport model for Hg (CTM-Hg) is used to investigate the sensitivity of global atmospheric Hg concentrations to various Hg emission scenarios. The emission scenarios are designed to reflect the best estimate of current uncertainties in Hg

* Corresponding author. Fax: +1 925 244 7124.
E-mail address: klohman@aer.com (K. Lohman).
[1] Currently: Graeagle, CA, USA.

0883-2927/$ - see front matter © 2008 Elsevier Ltd. All rights reserved.
doi:10.1016/j.apgeochem.2007.12.022

emissions. First a brief overview of the current status of Hg emissions estimates is presented. This was used as the base emission inventory within the CTM-Hg model. The base scenario follows that used in previous applications (Seigneur et al., 2004). Then, three emission scenarios are proposed and applied based on plausible emission estimate ranges for various source categories. The results of the global model simulations are presented for the base scenario and the three sensitivity scenarios. The simulated Hg concentrations are discussed in terms of their plausibility with respect to the understanding of realistic Hg concentrations. The uncertainties in Hg emissions can then be constrained and the scenarios that would require changes in atmospheric Hg chemistry (i.e., oxidation of elemental Hg (Hg^0) and reduction of Hg(II)) identified to obtain plausible results.

The first sensitivity scenario utilized the mid-range estimates from the literature for background emissions. Here "background emissions" are defined to include natural emissions and emissions of previously deposited Hg. The second sensitivity scenario utilized a higher load of anthropogenic Hg emissions to the atmosphere than previously estimated from China. The third sensitivity scenario combined increased rates of background emissions, as in the first sensitivity scenario, and doubled rates of all anthropogenic emissions to test an upper limit for emissions. Each simulation was analyzed for whether the results lead to atmospheric Hg^0 concentrations comparable to those found in the literature. Only Hg^0 concentrations were assessed, because Hg(II) and particulate Hg (Hg(p)) have shorter lifetimes than Hg^0 and their concentrations are influenced by local sources. The global model does not capture some of the high source-related concentrations of Hg(II) and Hg(p) due to potentially significant spatial gradients and the model's coarse spatial resolution.

2. The Model

The global CTM-Hg has been described by Seigneur et al. (2001, 2004). It provides a spatial resolution of 8° latitude and 10° longitude with seven layers in the troposphere and two layers in the stratosphere. The model is applied for one year using generic meteorological data obtained from a general circulation model and is run until steady state is achieved. The lifetime of Hg in the atmosphere is approximately one year. Elemental Hg is removed from the atmosphere by both dry deposition and oxidation, with oxidation of Hg^0 thought to be controlled by reactions with OH and O_3 (Seigneur et al., 2006). Mercury(II) is removed from the atmosphere through both wet and dry deposition as well as aqueous phase reactions with dissolved HO_2. Therefore, the atmospheric half-life of Hg(II) is much shorter (~1.6 days) than that of Hg(0) (~2 months) (Seigneur et al., 2006). The inputs to the global CTM-Hg used in this modeling exercise are identical to those presented by Seigneur et al. (2004) except for the emission estimates. Anthropogenic emissions and emissions of previously deposited Hg were updated to represent more recent estimates and are described in Table 1. Fifty percent of the Hg deposited is assumed to be emitted

Table 1
Global anthropogenic emission inventory for total Hg used in the CTM-Hg base simulation (2000 reference year)

Country/continent	Hg annual emissions (Mg/a)	$Hg^0/Hg^{II}/Hg_p$	References	Possible uncertainty
United States	104[a]	60/31/9	EPA (2004)	+70 Mg/a[b]
Canada	8	54/35/11	EPA (2004)	
Mexico	26[a]	71/20/9	CEC (2001)	× 1.8[c]
Asia	1204	57/34/9	Pacyna et al. (2003)	× 2[d]
Europe	239	61/32/7	Pacyna et al. (2003)	
South and Central America	92	71/23/6	Pacyna et al. (2003)	
Africa	407	65/28/7	Pacyna et al. (2003)	
Oceania	125	55/36/9	Pacyna et al. (2003)	
Total	2206			

[a] 1999 Inventory.
[b] +45 Mg/a of unaccounted Hg used in chlor-alkali plants (Southworth et al., 2004); +25 Mg/a of Hg emissions from motor vehicles (Edgerton and Jansen, 2004).
[c] Uncertainty factor derived from the range in Mexican emissions estimated by Pai et al. (2000).
[d] Estimate based on atmospheric Hg export estimates from Jaffe et al. (2005).

back to the atmosphere following Seigneur et al. (2004).

3. Emissions

3.1. Anthropogenic emissions

Since each Hg species has different deposition velocities and atmospheric reactions, the total emissions must be characterized by species emitted. Table 1 presents the estimated emissions and species on a regional basis. The anthropogenic emissions for the US and Canada are based on speciated EPA emission estimates for 2001 (EPA, 2004). The Mexican emission estimates are based on information from the Commission for Environmental Cooperation (CEC, 2001) on total Hg emissions from Mexican facilities. Because the Mexican data were only available as total Hg, speciation assumptions were made for each source category.

The continent contributing the most anthropogenic emissions is Asia. Asian emissions constitute the majority (55%) of the global 2000 anthropogenic emissions inventory (Table 1). The continent with the next largest contribution is Africa with 18% of the inventory. However, these emission estimates are highly uncertain due to lack of knowledge regarding sources and amounts of Hg emitted. Streets et al. (2005) estimate the emissions of Hg from China at 536 Mg/a for 1999 (compared to 586 Mg/a in the base inventory for 2000). In China, the largest source of emissions is estimated to be non-ferrous metal smelting (242 Mg/a) with coal combustion a close second (202 Mg/a) (Streets et al., 2005). The rest of the emissions are due to several small categories such as battery/fluorescent lamp production, cement production, Hg mining and biofuel combustion. The uncertainty of the Hg emission rate from China, however, is quite large (44%) (Streets et al., 2005), because for many of the emission categories activity levels and emission factors are not well characterized. Recent work by Pan et al. (2006), suggests that the uncertainty could in fact be as high as a factor of 2.

For other anthropogenic emissions, a database from the Meteorological Synthesizing Centre-East (MSC-E) for 2000 emissions was used as a starting point (Pacyna et al., 2006). The total emissions for each continent were scaled up or down so that they would reflect more recent estimates (Pacyna et al., 2003). The MSC-E database provided speciated emission estimates and the speciation ratios were maintained during scaling.

3.2. Background emissions

Table 2 summarizes the background emissions used in each simulation along with the range in emission estimates based on the literature. Mercury emitted either from natural sources or emitted after deposition from soil, vegetation or the oceans is assumed to be Hg^0. Emissions from the oceans were distributed according to a latitudinal gradient with greater emissions near the equator and lower emissions near the poles (Kim and Fitzgerald, 1986).

Natural emissions in the inventory come from three sources: mercuriferous soils, volcanoes and ocean emissions. All of these sources have uncertainties associated with their emission estimates. Additionally, some sources may be missing from the base inventory.

Volcanic emissions may be significantly underestimated based on the emissions inventory reported by Pyle and Mather (2003). The uncertainty range spans nearly three orders of magnitude but the more likely estimates seem to be in the range of 90–830 Mg/a (Pyle and Mather, 2003).

Land-based natural emissions are due predominantly to mercuriferous soils. Mercuriferous soils have been well characterized in Nevada (e.g., Zehner and Gustin, 2002), but the extrapolation of those values to the globe involves significant uncertainties. Gustin and Lindberg (2005) estimated that emissions due to mercuriferous soils could exceed 1500 Mg/a. Emissions from other soils are likely to include both low natural emissions and emission of previously deposited Hg, which could be of either anthropogenic or natural origin. There are few extensive measurements of Hg emissions from background soil. Atmospheric Hg exchange with substrates is bi-directional. Both emission and deposition are important fluxes (Lindberg et al., 1998; Engle et al., 2001; Zhang et al., 2001; Nacht and Gustin, 2004; Ericksen et al., 2005, 2006; Gustin et al., 2006). One recent study (Ericksen et al., 2005) suggested a flux of 0.5–1 ng/m^2 h for soils (which could be scaled to give a global range of 500–1000 Mg/a), however, they suggested that this flux could just reflect emission of Hg previously deposited by wet and dry processes. Therefore, potential direct natural emissions from background soil were not included in the base scenario natural emission estimate. Only emissions of previously

deposited Hg were used for emissions from background soils.

While emissions from geothermal power plants were included in the anthropogenic inventory, emissions from other geothermal areas were not explicitly included in the base simulation. Gustin and Lindberg (2005) provide a global estimate of 60 Mg/a based on Varenkamp and Buseck (1984). Engle et al. (2006a) recently estimated annual Hg emissions from active hydrothermal systems in the conterminous United States to be 1.3–2.1 Mg and suggested that this estimate supported the Varenkamp and Buseck (1984) global estimate.

In the base scenario, several natural Hg emission categories were included under the umbrella of emission of previously deposited Hg. Among these were emissions from vegetation, biomass fires, wetlands and snow. A few of these categories have some information on which to base emission estimates. Few data are available for Hg emissions from vegetation at the global scale. Gustin and Lindberg (2005) report data ranging from 850 to 2000 Mg/a for forests (Lindberg et al., 1998). It is thought, however, that plant foliage is dominantly a sink for atmospheric Hg; however, the leaf surface is a dynamic surface of exchange where deposition and emission of Hg can occur (Millhollen et al., 2006). Emissions from biomass fires were estimated by Friedli et al. (2003a) to be in the range of 100–850 Mg/a, while Friedli et al. (2003b) and Engle et al. (2006b) gave estimates for the conterminous United States of 1.5–5.5 Mg/a. Wetlands, snow and freshwater bodies have not been individually estimated and must remain part of the category of

Table 2
Summary of global background emissions: ranges of uncertainties (all emissions are in Mg/a)

Emission source	Base Scenario[a]	Scenario 1	Scenario 2	Scenario 3	Range from literature	References
Volcanoes	125	700	125	700	1–830	Pyle and Mather (2003)
Soils (mercuriferous)	500	1000	500	1000	500–1500	Zehner and Gustin (2002)
Soils (emissions of prev. dep. Hg)	1700[c]	750	1700[c]	750	500–1000[b]	Ericksen et al. (2006)
Vegetation (direct emissions)	0	0	0	0	1650–4300	Lindberg et al. (1998), Obrist et al. (2004)
Vegetation (emissions of prev. dep. Hg)	0[d]	0[d]	0[d]	0[d]		
Geothermal areas	0	60	0	60	60	Varenkamp and Buseck (1984)
Freshwater	0[d]	0[d]	0[d]	0[d]	–	Poissant et al. (2000)
Wetlands	0[d]	0[d]	0[d]	0[d]	–	Lindberg et al. (2002)
Snow	0[d]	0[d]	0[d]	0[d]	–	Lalonde et al. (2002)
Biomass fires	0[d]	500	0[d]	500	100–850	Friedli et al. (2003a)
Oceans (direct emissions/ emissions of previously deposited Hg)	2010 (440/ 1570)	2010 (440/ 1570)	2010 (440/ 1570)	2010 (440/ 1570)	600–2600 (0–1300[e]/600[f]–1300[e])	Lamborg et al. (2002), Mason and Sheu (2002)

[a] Nominal values from Seigneur et al. (2004) with revisions to anthropogenic emissions of previously deposited Hg to reflect 2000 values.
[b] The global estimate values were obtained by scaling flux measurements from Gustin et al. (2006) to the global land area.
[c] Emissions of previously deposited Hg were assumed to be 50% of the amount of deposited Hg globally.
[d] These emissions were assumed to be already included in the re-emissions from land.
[e] The flux out of the marine boundary layer is estimated as 730 Mg/a (i.e., 570 Mg/a of Hg^0 is oxidized and deposited within the boundary layer.
[f] Re-emissions of natural Hg only, Lamborg et al. (2002).

emissions of previously deposited Hg. Wetlands can act as either a source or a sink of Hg (Poissant et al., 2004a, b; Lindberg et al., 2002). Mercury deposited due to snowfall may be re-emitted into the atmosphere (Lalonde et al., 2002). Emissions of Hg from freshwater bodies are mostly due to emissions of Hg that enters the water body via atmospheric deposition to the watershed and the water body or direct discharge to the water body (e.g., Vette et al., 2002).

Emissions from oceans were estimated to be about 2000 Mg/a in the CTM-Hg base simulation. Lamborg et al. (2002) estimated that ocean emissions were only 600 Mg/a with the entire amount corresponding to emissions of previously deposited Hg. Mason and Sheu (2002) estimated a total flux of 2600 Mg/a, which was equally distributed between natural emissions and emissions of anthropogenic Hg deposited to the oceans (natural emissions included both direct emissions and emissions of deposited natural Hg). However, Mason and Sheu (2002) estimated that only half of that flux would reach the free troposphere and that half of Hg^0 emitted in the marine boundary layer would be rapidly oxidized to Hg(II) and would deposit back to the oceans.

4. Results

4.1. Base simulation

Fig. 1 depicts the annual average surface concentrations of Hg^0 simulated with the global CTM-Hg for the base scenario. The results are similar to those presented by Seigneur et al. (2004). Minor differences in the results are due to changes in the anthropogenic emission inventory. The current inventory differs by 3% on average from that used in the previous study. Those simulation results were shown to be consistent overall with available observations for Hg^0 (Seigneur et al., 2004).

Fig. 2 depicts a comparison between measured total gaseous Hg measurements taken at latitudes across the northern and southern hemispheres in the Atlantic Ocean (Temme et al., 2003) and modeled results over the same area for each scenario. Fig. 3 presents the path of the ship cruise

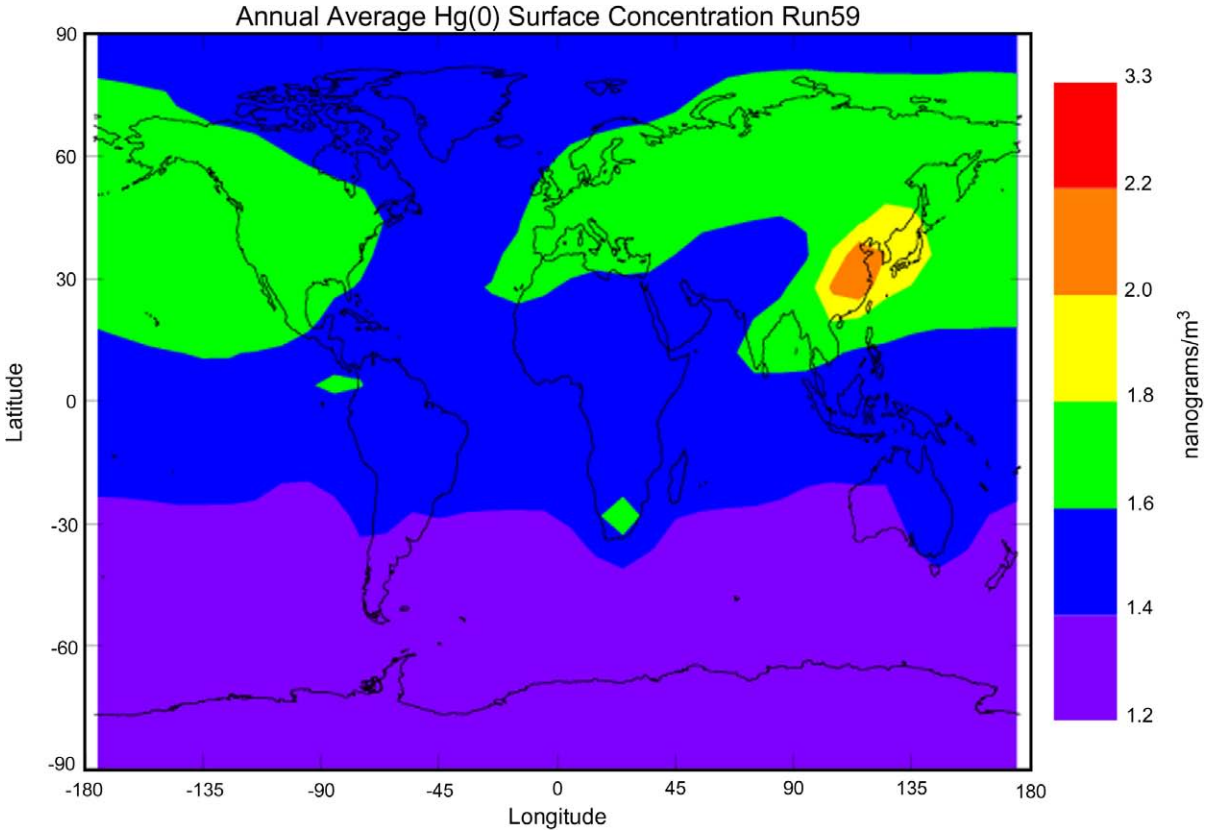

Fig. 1. Global Hg^0 concentrations in ng/m^3 for the base simulation.

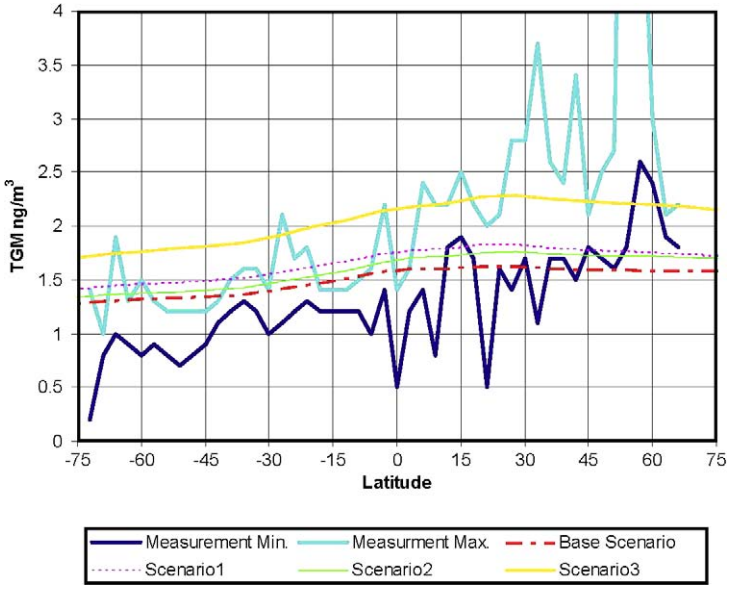

Fig. 2. Comparison of measured Temme et al. (2003) and modeled total gaseous mercury (TGM) over the Atlantic Ocean.

corresponding to those measurements. The model reproduces well the North-South gradient in Hg^0 concentrations and the model predictions fall within the lower and upper bounds of the measurements except at the mid-latitudes in the northern hemisphere (55–60° North), where the measurements were probably affected by regional anthropogenically affected air masses. Table 4 provides a comparison of measurements in different regions of the world at remote sites from the literature (Valente et al., 2006) with annually averaged Hg^0 concentrations from the corresponding grid cells in each modeling scenario. Fig. 3 shows the locations of the measurements presented in Table 4. The range of values produced by the model for the eastern North American, western North American, northern European and Arctic regions are within the range of the measurements in those locations. The results for the western European and Japanese locations were slightly underestimated (less than 10%), while the result for the Antarctic site was overestimated by a much larger amount (30%).

4.2. Sensitivity to natural emissions

Natural emissions in the base scenario inventory come from three sources: mercuriferous soils, volcanoes and ocean emissions. All of these sources have uncertainties associated with their emission estimates. Additionally, some sources may be missing from the base inventory. In this sensitivity scenario the impact of these uncertainties are studied.

The sum of natural emissions and emissions of previously deposited Hg from land and oceans in the base simulation is about 4300 Mg/a. Using the mid-range value of the emissions estimates from volcanoes, mercuriferous soils, other soils, geothermal areas, vegetation and biomass fires (see Table 3) would lead to an estimate of about 8000 Mg/a, i.e., 1.8 times the base scenario. Using the upper range of the emissions from volcanoes, mercuriferous soils, other soils, geothermal areas, vegetation and biomass fires, and leaving emissions from oceans unchanged would lead to an estimate of about 10,500 Mg/a, i.e., 2.4 times the base scenario (emissions from oceans remaining equal to their base scenario values). However, such emission scenarios would have a ratio of current emissions/pre-industrial emissions less than two. This is thought to be unrealistic, because available lake sediment data suggest a range of 2–4 for this ratio (Lindberg et al., 2007, and references therein).

Based on the above estimates and assuming a current emission to pre-industrial emission ratio of 2–4, a sensitivity scenario (Scenario 1) was designed that would allow investigation of the impact of increased background emissions. This sensitivity scenario takes into account uncertainties in the natural emissions and emissions of previously deposited Hg. For this scenario, the mid-range value

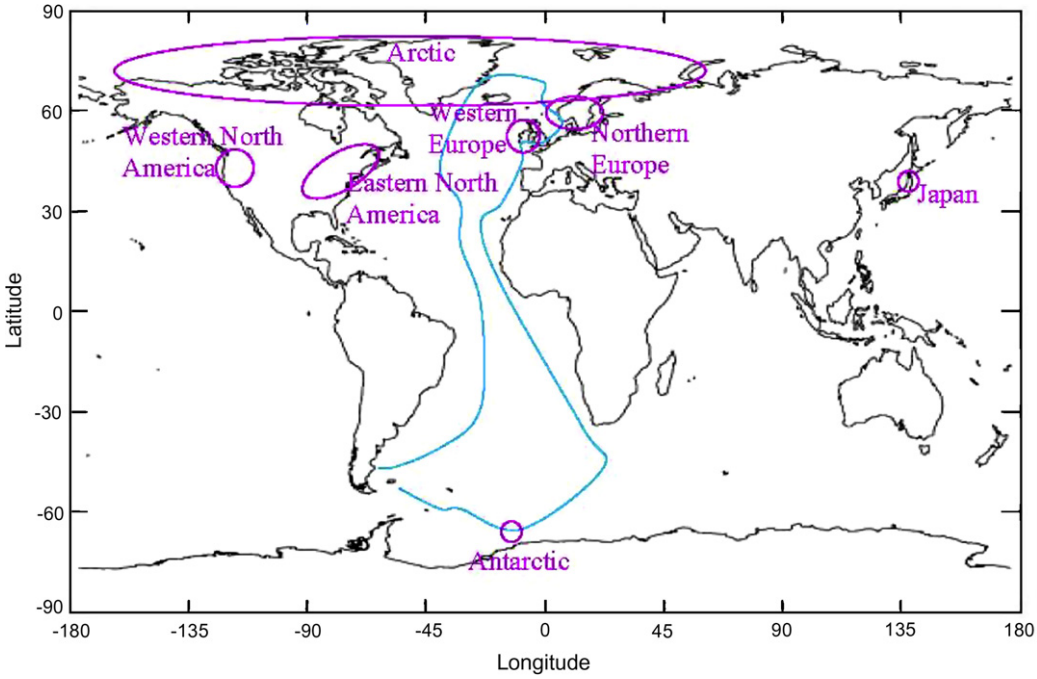

Fig. 3. Map of locations of measurements of Hg^0 used to compare against modeled data (see Table 4).

from the literature (shown in Table 3) was used in place of the corresponding values for each land-based background emission category. This leads to an increase of 1135 Mg/a in natural emissions. However, emissions of previously deposited Hg decreased by 452 Mg/a, because the addition of emissions from biomass fires was less than the change made to emissions from background soils (emissions from background soils decreased due to the overall constraint placed on total natural emissions). This leads to a net increase in overall background emissions of 683 Mg/a, i.e., 16%.

Fig. 4 depicts the global Hg^0 concentrations resulting from this sensitivity case. The results show slightly higher concentrations than the base simulation but still appear realistic (see Table 3). Modeled Hg^0 concentrations increased around the world compared to those from the base simulation anywhere from 6–24%. Clear north-south gradients are still visible and the concentrations in the Northern Hemisphere range from 1.6 to 2.3 ng/m^3 (see Fig. 4). When comparing the model simulation results with measurements at remote sites (see Table 4), it appears that the model results are now higher in all of the regions than in the base scenario. Only the results for the eastern North American and Arctic regions still fall within the measured range. Agreement at the Japanese site has improved (2%), but worsened at the Antarctic site (40%). Modeled results in Western Europe are now overestimated but by approximately the same amount as they were underestimated in the base scenario. In summary, model performance improved at some sites but degraded at others; overall, this emission scenario still provides Hg^0 concentrations that are consistent with the observational record.

4.3. Sensitivity to anthropogenic emissions from China

This emission scenario (Scenario 2) addresses the hypothesis that Chinese industrial Hg^0 emissions are underestimated (Jaffe et al., 2005). This hypothesis attempts to explain the large atmospheric flux of Hg out of Asia as estimated from measurements both in coastal Washington State and in Okinawa by Jaffe et al. (2005). In this emission scenario, anthropogenic emissions from China were increased from those in the base simulation; Hg speciation ratios were maintained from the base simulation. In the base emission inventory, anthropogenic Hg emissions from China amount to 586 Mg/a. A recent emission inventory conducted by Streets et al. (2005) for 1999 reports an estimate of 536 Mg/a with an uncertainty of 44% (95% confidence interval); therefore, their upper limit is 772 Mg/a. However, Pan

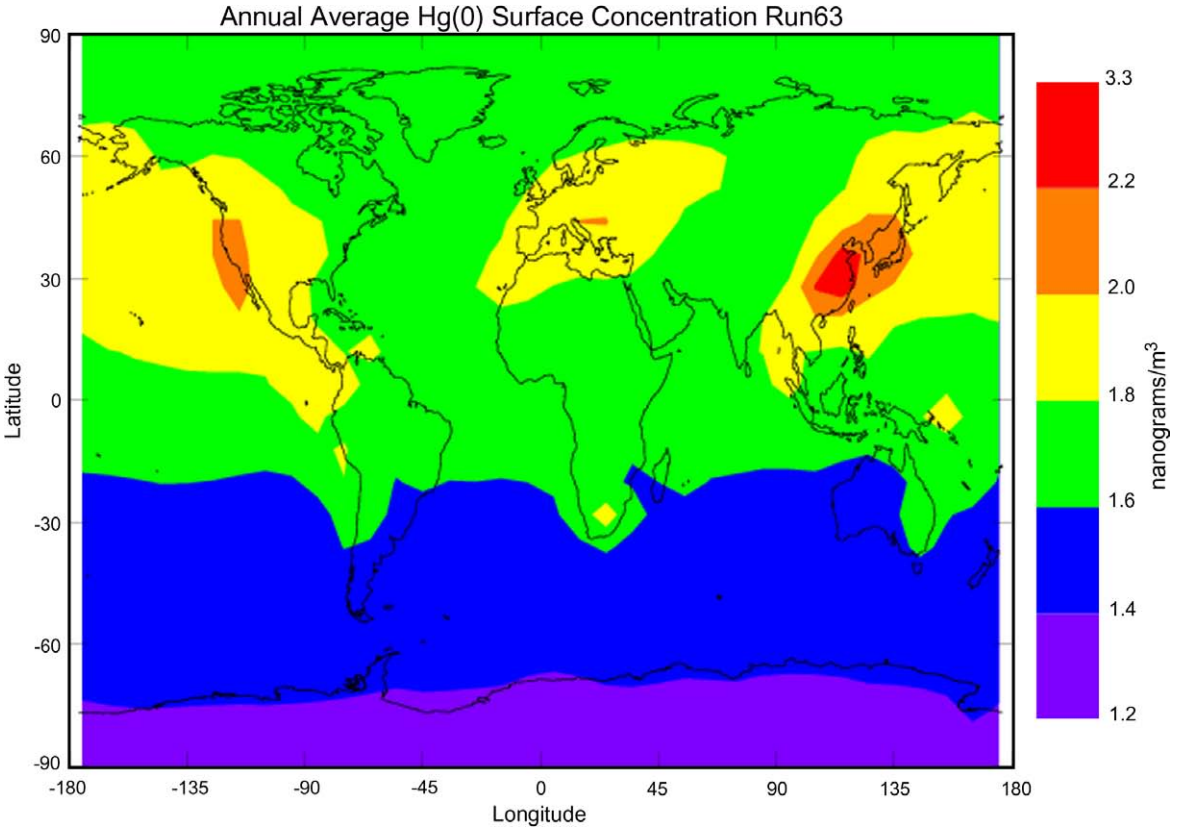

Fig. 4. Global Hg^0 concentrations in ng/m^3 for the background emission increase simulation (Scenario 1).

Table 3
Summary of the emission scenarios (emissions by source category are rounded-off to nearest 100 Mg/a)[a]

Emissions	Base scenario	Sensitivity scenario 1	Sensitivity scenario 2	Sensitivity scenario 3
Anthropogenic emissions (Mg/a)	2200	2200	2800	4400
Natural emissions (Mg/a)	1100	2200	1100	2200
Emissions of previously deposited Hg (Mg/a)	3300	2800	3300	2800
Total emissions (Mg/a)	6600	7200	7200	9400
Ratio of current/pre-industrial emissions	3.1	2.0	3.6	3.0
Fraction of deposited Hg being re-emitted globally[b]	50%	39%	46%	30%
Range of simulated Hg^0 concentrations (ng/m^3)	1.2–2.2	1.4–2.3	1.3–2.8	1.6–3.2

[a] Emission information has been rounded to two significant digits.
[b] See text regarding assumptions for natural versus emissions of previously deposited Hg.

Table 4
Comparison of measurements and modeled Hg^0 concentrations (ng/m^3) for the four scenarios (see Fig. 3)

Site	Hg^0 (ng/m^3)	Base (ng/m^3)	Scenario 1 (ng/m^3)	Scenario 2 (ng/m^3)	Scenario 3 (ng/m^3)
Eastern North America	1.50–1.83	1.60–1.65	1.75–1.82	1.73–1.78	2.25–2.42
Western North America	1.43–1.77	1.69–1.70	1.94–2.00	1.83–1.85	2.44–2.52
Western Europe	1.72–1.75	1.62	1.80	1.75	2.32
Northern Europe	1.35–1.76	1.61–1.64	1.78–1.95	1.74–1.76	2.33–2.38
Japan	2.04	1.87	2.09	2.14	2.92
Arctic	1.32–1.80	1.53–1.64	1.66–1.79	1.64–1.76	2.11–2.29
Antarctic	0.99	1.29	1.41	1.35	1.71

et al. (2006) estimated a larger uncertainty for Chinese emissions, by a factor of two. Accordingly, in this emission scenario, the base anthropogenic emission for China were doubled to 1172 Mg/a. Such a value should provide an upper bound for Chinese anthropogenic emissions, even accounting for growth and uncertainty. All other emission sources remained the same as in the base scenario. Using this increase in the Chinese emissions, there is a current/pre-industrial emission ratio of 3.6, which is within current estimates.

Fig. 5 depicts the global Hg^0 concentrations resulting from this sensitivity case. The Northern Hemisphere Hg^0 concentrations are higher than in the base simulation. Northern Hemisphere concentrations range from 1.6 to 2.8 ng/m^3. The patterns of high concentration are still similar and the north-south gradient is still readily apparent (see Fig. 2). The modeled Hg^0 concentrations in this sensitivity scenario increased around the world over those from the base simulation from 3 to 29%. Comparison of model simulation results with measurements at remote sites (see Table 4) shows that this scenario leads to Hg^0 concentrations that are slightly lower than those obtained in the previous scenario in all regions except Japan. The modeling results in all regions are higher than in the base scenario. Consequently, model performance improved at some sites compared to the base simulation but degraded at other sites. Overall, these results suggest that greater Hg emissions from Chinese anthropogenic sources are not incompatible with the global constraints placed by measured Hg^0 concentrations and that the uncertainty ranges given by Streets et al. (2005) and Pan et al. (2006) are commensurate with a plausible global Hg cycling scenario.

4.4. Sensitivity to increased background and anthropogenic emissions

Scenario three was created to address uncertainties associated with anthropogenic emission estimates. It has been suggested based on research at US facilities that emissions from certain source categories such as chlor-alkali plants may be

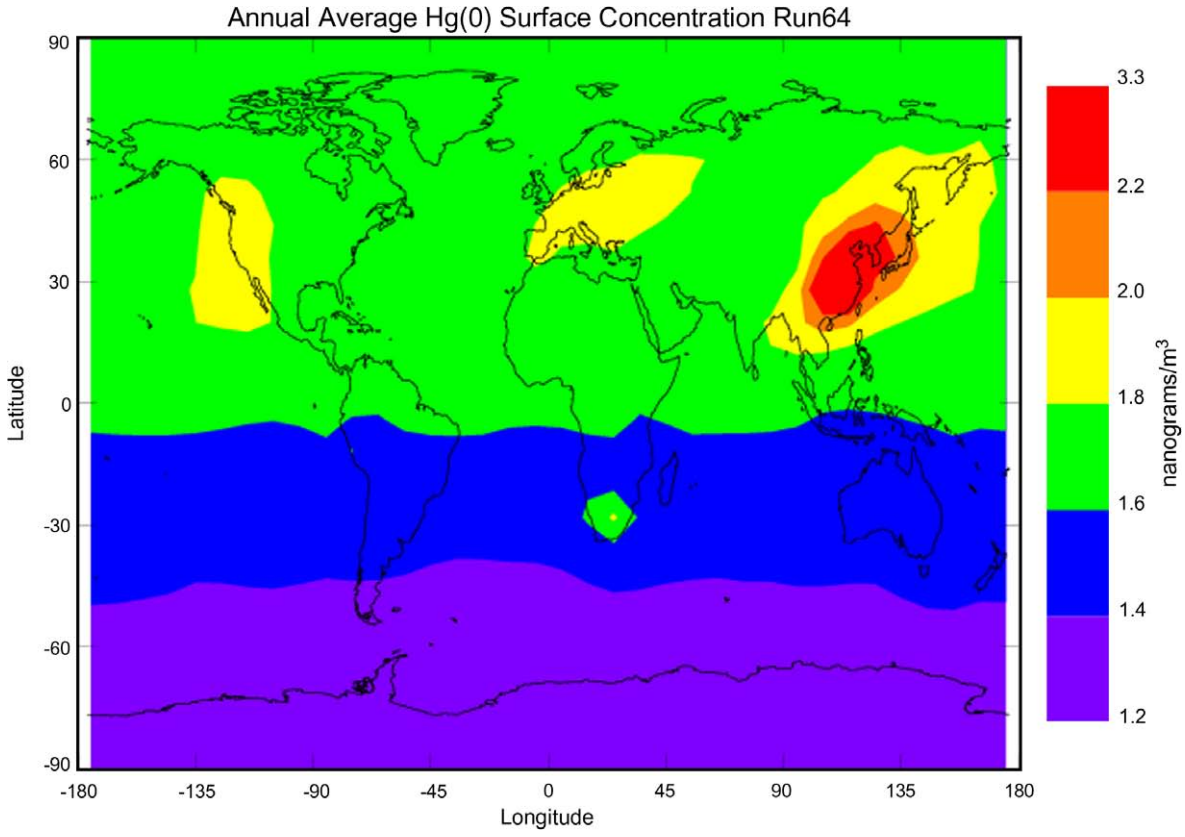

Fig. 5. Global Hg^0 concentrations in ng/m^3 for the Chinese emissions increase simulation (Scenario 2).

underestimated (Southworth et al., 2004; Lindberg et al., 2004). In addition, there are source categories that are not accounted for in Hg emission inventories but may be significant. One example includes automobile emissions. Measurements of Hg and CO, a tracer for mobile source emissions in urban areas in Atlanta, GA, USA, suggested that mobile sources could be a significant source of Hg^0 (Edgerton and Jansen, 2004). Similarly, analysis of Hg concentrations in Detroit, MI, USA, using principal component analysis (PCA) identified mobile sources as a significant Hg source category (Lyman and Keeler, 2006). Mobile sources are included in the US emission inventory but are not included in the emission inventories of other countries. This could lead to an uncertainty of up to 20% based on the US inventory. Uncertainties in overall anthropogenic Mexican emissions were estimated by Pai et al. (2000) to be about a factor of 1.8. As discussed above, recent reported data on the export of atmospheric Hg from Asia suggest that Asian anthropogenic emissions could be underestimated by a factor of 2 (Jaffe et al., 2005). Based on these few estimates of uncertainties in anthropogenic emissions, an upper bound of a factor of 2 was selected for the anthropogenic emission uncertainty for Scenario 3. This emission scenario uses the same background emissions as in the first sensitivity scenario and also doubles the global anthropogenic emissions. This scenario can be considered a plausible upper bound for Hg emissions.

The results of this scenario are shown in Fig. 6. The maximum concentration of Hg^0 is now up to 3.2 ng/m^3. The modeled Hg^0 concentrations increased from the base simulation by a minimum of 28% and a maximum of 51%. The results from this simulation do not agree as well with observations as those from the other sensitivity scenarios (see Table 3). The north-south gradient has been disrupted (see Fig. 2) and is not consistent with the observations (Slemr and Langer, 1992; Slemr et al., 1995). Comparison of model simulation results with measurements at remote sites (see Table 4) shows that the model overestimates by at least 0.4 ng/m^3 in all regions and that, therefore, the modeled concentrations are not realistic.

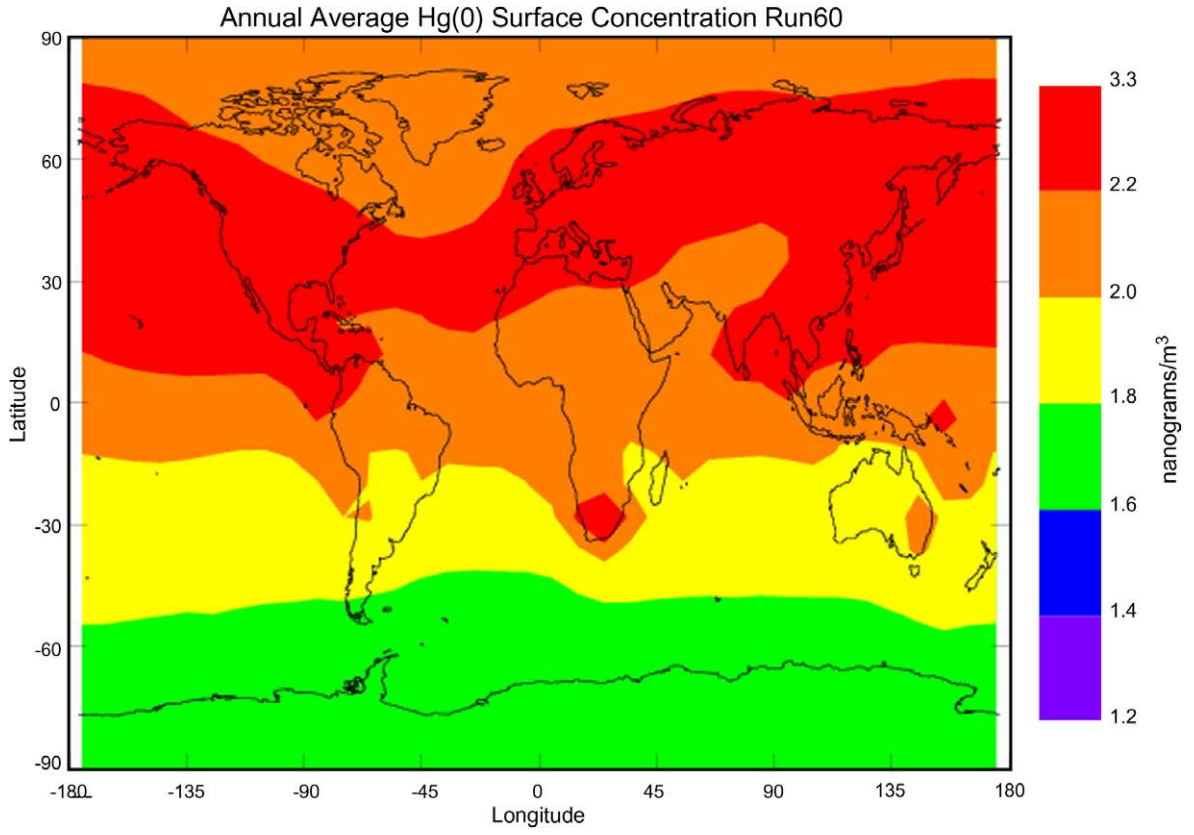

Fig. 6. Global Hg^0 concentrations in ng/m^3 for the upper bound emission simulation (Scenario 3).

Such an emission scenario cannot, however, be ruled out. Seigneur et al. (2006) demonstrated that uncertainties in the reduction and oxidation (red–ox) reactions of Hg species could affect Hg^0 concentrations and that doubling Hg emissions led to realistic results, if slower Hg(II) reduction kinetics were used. In addition, the potential for soils and plants to act as sinks for atmospheric elemental Hg was not considered in the model simulation (Millhollen et al., 2006; Gustin et al., 2006; Gustin and Lindberg, 2005).

5. Conclusions

The impact of uncertainty in the global Hg emission inventory was investigated with a global chemical transport model. A base simulation reflecting "best estimates" used in earlier work was the base simulation. Three sensitivity simulations reflecting uncertainty over different categories of emissions were run. The first increased global natural emissions with a net increase in overall background emissions of 16%. The second doubled anthropogenic emissions from China. The third applied the 16% increase in background emissions from the first sensitivity simulation and also doubled all anthropogenic emissions. The base simulation and the first two sensitivity simulations all produce results that are compatible with observations. The discussions of current Hg emissions as well as the sensitivity scenarios demonstrate both that the current emission estimates have a high degree of uncertainty and that these uncertainties are within the constraints imposed by the available measurements of Hg^0 concentrations. On the other hand, the third sensitivity scenario demonstrates that increasing background emissions by 16% and doubling anthropogenic emissions produces unrealistic results. However, such a scenario cannot be ruled out because of current uncertainties in the atmospheric chemistry of Hg. For example, if a slower rate of atmospheric Hg(II) reduction is used and soils and vegetation act as significant sinks for Hg^0 then the model results might be consistent with observations.

In summary, current anthropogenic emissions are uncertain by about a factor of 2 based on comparison with ambient concentrations. Since the ratio of current to pre-industrial emissions is constrained within a range of 2–4, natural emissions are constrained by a factor of 4 uncertainty. Therefore, assuming a maximum fraction of 50% for the emissions of previously deposited Hg to the atmosphere, an overall uncertainty in total Hg emissions can be placed at a factor of 2–3. The current uncertainty in total Hg emissions at the global scale is placed at about a factor of 2. Reducing those uncertainties will require more accurate emission inventories of anthropogenic sources, particularly for countries that have been identified as large Hg emitters (e.g., China) and for source categories that are not currently included in emission inventories but could be significant (e.g., mobile sources). In addition, better characterization of background emissions (i.e., both natural emissions and the emissions of previously deposited Hg) is needed. Finally, constraining the global Hg cycle will only be possible if a more precise understanding of the Hg atmospheric chemical cycle is developed in parallel.

Acknowledgements

Atmospheric and Environmental Research, Inc. performed this work under contract with EPRI (Contract No. EP-P20954/C10205). Thanks are due to the EPRI Project Manager, Dr. Leonard Levin, for his continuous support throughout this study.

References

Bergan, T., Gallardo, L., Rohde, H., 1999. Mercury in the global troposphere: a three-dimensional model study. Atmos. Environ. 33, 1575–1585.

CEC, 2001. Preliminary atmospheric emissions inventory of mercury in Mexico. Report No. 3.2.1.04, Commission for Environmental Cooperation, Montreal, Canada.

Edgerton, E.S., Jansen, J.J., 2004. Elemental Hg measurements in Atlanta, GA, USA: evidence for mobile sources. In: Proceedings of the 7th International Conference Mercury as a Global Pollutant, 27 June–2 July 2004, Ljubljana, Slovenia, RMZ – Materials and Geoenvironment 51, 1540.

Engle, M.A., Gustin, M.S., Goff, F., Counce, D.A., Janik, C.J., Bergfeld, D., Rytuba, J.R., 2006a. Atmospheric mercury emissions from substrates and fumaroles associated with three hydrothermal systems in the Western United States. J. Geophys. Res. 111, D17304.

Engle, M.A., Gustin, M.S., Johnson, D.W., Murphy, J., Wright, J., Markee, M., 2006b. Mercury distribution in two Sierran forest and one desert sagebrush ecosystem and the effects of fire. Sci. Tot. Environ. 367, 222–233.

Engle, M.A., Gustin, M.S., Zhang, H., 2001. Quantifying natural source mercury emissions from the Ivanhoe Mining District, north-central Nevada, USA. Atmos. Environ. 35, 3987–3997.

EPA, 2004. Emissions data for US and Canadian point and area sources. Pers. Comm., Marc Houyoux, US Environmental Protection Agency, Research Triangle Park, NC.

Ericksen, J., Gustin, M., Lindberg, S., Olund, S., Krabbenhoft, D., 2005. Assessing the potential for re-emission of mercury

deposition in precipitation from arid soils using a stable isotope. Environ. Sci. Technol 39, 8001–8007.
Ericksen, J.A., Gustin, M.S., Xin, M., Weisberg, P.J., Fernandez, G.C.J., 2006. Air–soil exchange of mercury from background soils in the United States. Sci. Tot. Environ. 366, 851–863.
Friedli, H.R., Radke, L.F., Lu, J.Y., Banic, C.M., Leaitch, W.R., MacPherson, J.J., 2003a. Mercury emissions from burning of biomass from temperate North American forests: laboratory and airborne measurements. Atmos. Environ. 37, 253–267.
Friedli, H.R., Radke, L.F., Prescott, R., Hobbs, P.V., Sinha, P., 2003b. Mercury emissions from the August 2001 wildfires in Washington State and an agricultural waste fire in Oregon and atmospheric mercury budget estimates. Global Biogeochem. Cycles 17, 1039. doi:10.1029/2002GB1972.
Gustin, M.S., Lindberg, S.E., 2005. Terrestrial mercury fluxes: Is the net exchange up, down or neither? In: Pironne, N., Mahaffey, K. (Eds.), Dynamics of Mercury Pollution on Regional and Global Scales: Atmospheric Processes, Human Exposure Around the World. Springer Publisher, Nowell, MA, pp. 41–260 (Chapter 11).
Gustin, M.S., Engle, M.A., Ericksen, J., Lyman, S., Stamenkovic, J., Xin, M., 2006. Elemental Hg exchange between the atmosphere and low Hg containing substrates. Appl. Geochem. 21, 1913–1923.
Jaffe, D., Prestbo, E., Swartzendruber, P., Weiss-Penzias, P., Kato, S., Takami, A., Hatakeyama, S., Kajii, Y., 2005. Export of atmospheric mercury in Asia. Atmos. Environ. 39, 3029–3038.
Kim, J.P., Fitzgerald, W.F., 1986. Sea-air partitioning of mercury in the equatorial Pacific Ocean. Science 231, 1131–1133.
Lalonde, J.D., Poulain, D.J., Amyot, M., 2002. The role of mercury redox reactions in snow on snow-to-air mercury transfer. Environ. Sci. Technol. 36, 174–178.
Lamborg, C.H., Fitzgerald, W.F., Damman, A.W.H., Benoit, J.M., Balcom, P.H., Engstrom, D.R., 2002. Modern and historic atmospheric mercury fluxes in both hemispheres: global and regional mercury cycling implications. Global Biogeochem. Cycles 16, 1104. doi:10.1029/2001GB1847.
Lindberg, S., Bullock, O.R., Ebinghaus, R., Engstrom, D., Feng, X., Fitzgerald, W., Pirrone, N., Prestbo, E., Seigneur, C., 2007. A synthesis of progress and uncertainties in attributing the sources of mercury in deposition. Ambio 36, 19–32.
Lindberg, S., Dong, W., Meyers, T., 2002. Transpiration of gaseous elemental mercury through vegetation in a subtropical wetland in Florida. Atmos. Environ. 36, 5207–5219.
Lindberg, S.E., Hanson, P.J., Meyersand, T.P., Kim, K.-H., 1998. Air/surface exchange of mercury vapor over forests: the need for a reassessment of continental biogenic emissions. Atmos. Environ. 32, 895–908.
Lindberg, S., Porcella, D., Prestbo, E., Friedli, H., Radke, L., 2004. The problem with mercury: too many sources, not enough sinks. In: Proceedings of the 7th International Conference Mercury as a Global Pollutant, 27 June–2 July 2004, Ljubljana, Slovenia, RMZ – Materials and Geoenvironment 51, pp. 1172–1176.
Lyman, M.M., Keeler, G.J., 2006. Source receptor relationships for atmospheric mercury in urban Detroit, MI. Atmos. Environ. 40, 3144–3155.
Mason, R.P., Sheu, G.-R., 2002. Role of the ocean in the global mercury cycle. Global Biogeochem. Cycles 16, 1093. doi:10.1029/2001GB1440.
Millhollen, A., Gustin, M.S., Obrist, D., 2006. Foliar mercury accumulation and exchange for three tree species. Environ. Sci. Technol. 40, 6001–6006.
Nacht, D.M., Gustin, M.S., 2004. Mercury emissions from background and altered geologic units throughout Nevada. Water Air Soil Pollut. 151, 179–193.
Obrist, D., Gustin, M.S., Arnone, J.A., Johnson, D.W., Schorran, D.E., Verburg, P.J., 2004. Large annual mercury emissions to the atmosphere over Tallgrass Prairie ecosystems. Atmos. Environ. 39, 957–965.
Pacyna, J., Pacyna, E., Steenhuisen, F., Wilson, S., 2003. Global Mercury Emissions, Long Range Transport Workshop, 16–17 September 2003, Ann Arbor, MI.
Pacyna, E., Pacyna, J., Steenhuisen, F., Wilson, S., 2006. Global anthropogenic mercury emission inventory for 2000. Atmos. Environ. 40, 4048–4063.
Pai, P., Niemi, D., Powers, B., 2000. A North American inventory of anthropogenic mercury emissions. Fuel Process. Technol. (65–66), 101–115.
Pan, L., Chai, T., Carmichael, G.R., Tang, Y., Streets, D., Woo, J-H., Friedli, H.R., Radke, L.F., 2006. Top-down estimate of mercury emissions in China using four-dimensional variational data assimilation. Atmos. Environ. 41, 2804–2819.
Poissant, L., Amyot, M., Pilote, M., Lean, D., 2000. Mercury water–air exchange over the upper St. Lawrence river and Lake Ontario. Environ. Sci. Technol. 34, 3069–3078.
Poissant, L., Pilote, M., Constant, P., Beauvais, C., Zhang, H.H., Xu, X., 2004a. Mercury gas exchanges over selected bare soils and flooded sites in the Bay St. François wetlands (Québec, Canada). Atmos. Environ. 38, 4205–4214.
Poissant, L., Pilote, M., Xu, X., Zhang, H., Beauvais, C., 2004b. Atmospheric mercury speciation and deposition in the Bay St. François wetlands. J. Geophys. Res. 109. doi:10.1029/2003/D004364.
Pyle, D.M., Mather, T.A., 2003. The importance of volcanic emissions for the global atmospheric mercury cycle. Atmos. Environ. 37, 5115–5124.
Seigneur, C., Karamchandani, P., Lohman, K., Vijayaraghavan, K., Shia, R.-L., 2001. Multiscale modeling of the atmospheric fate and transport of mercury. J. Geophys. Res. 106, 27795–27809.
Seigneur, C., Vijayaraghavan, K., Lohman, K., 2006. Atmospheric mercury chemistry: sensitivity of global model simulations to chemical reactions. J. Geophys. Res. 111, D22306. doi:10.1029/2005JD006.
Seigneur, C., Vijayaraghavan, K., Lohman, K., Karamchandani, P., Scott, C., 2004. Global source attribution for mercury deposition in the United States. Environ. Sci. Technol. 38, 555–569.
Slemr, F., Langer, E., 1992. Increase in global atmospheric concentrations of mercury inferred from measurements over the Atlantic Ocean. Nature 355, 434–437.
Slemr, F., Junkermann, W., Schmidt, R.W.H., Sladkovic, R., 1995. Indication of change in global and regional trends of atmospheric mercury concentrations. Geophys. Res. Lett. 22, 2143–2146.
Southworth, G.R., Lindberb, S.E., Zhang, H., Kinsey, J.S., Anscombre, F., Schaedlich, F., 2004. Fugitive mercury emissions from a chlor-alkali facility: sources and fluxes to the atmosphere. Atmos. Environ. 38, 633–641.

Streets, D.G., Hao, J., Wu, Y., Jiang, J., Chan, M., Tian, H., Fengm, X., 2005. Anthropogenic mercury emissions in China. Atmos. Environ. 39, 7789–7806.

Temme, C., Slemr, F., Ebinghaus, R., Einax, J.W., 2003. Distribution of mercury over the Atlantic Ocean in 1996 and 1999–2001. Atmos. Environ. 37, 1889–1897.

Valente, R., Shea, C., Humes, K.L., Tanner, R., 2006. Atmospheric mercury in the Great Smoky Mountains compared to regional and global levels. Atmos. Environ. 41, 1861–1873.

Varenkamp, J.C., Buseck, P.R., 1984. The speciation of mercury in hydrothermal systems with applications to ore deposition. Geochimi. Cosmochimi. Acta 48, 177–185.

Vette, A.F., Landis, M.S., Keeler, G.J., 2002. Deposition and emission of gaseous mercury to and from Lake Michigan during the Lake Michigan Mass Balance Study. Environ. Sci. Technol. 36, 4525–4532.

Zehner, R.E., Gustin, M.S., 2002. Estimation of mercury vapor flux from natural substrate in Nevada. Environ. Sci. Technol. 36, 4039–4045.

Zhang, H., Lindberg, S.E., Marsik, F.J., Keeler, G.J., 2001. Mercury air/surface exchange kinetics of background soils of the Tahquamenon River watershed in the Michigan Upper Peninsula. Water Air Soil Pollut. 126, 151–169.